JCTC Journal of Chemical Theory and Computation

Mechanisms for the Reactions of Hydroxyl Radicals with Acrolein: A Theoretical Study

Santiago Olivella*,† and Albert Solé‡

Institut d'Investigacions Químiques i Ambientals de Barcelona, CSIC, Jordi Girona 18-26, 08034-Barcelona, Catalonia, Spain, and Departament de Química Física i Institut de Recerca en Química Teòrica i Computacional, Universitat de Barcelona, Martí i Franquès 1, 08028-Barcelona, Catalonia, Spain

Received March 6, 2008

Abstract: Three low-energy pathways for the reaction of HO• with acrolein, a key reaction in atmospheric environments, have been investigated by means of quantum-mechanical electronic structure methods (UQCISD and RQCISD(T)). The first step of all the reaction pathways studied involves the barrierless formation of a prereaction loosely bound complex in the entrance channel, lying a few kcal/mol below the energy of the reactants. The lowest-energy barrier pathway at 0 K is found to be the HO• abstraction of the aldehydic H-atom through a transition-state structure lying 1.1 kcal/mol below the energy of the reactants. The addition of HO• to the terminal carbon atom of the C═C double bond proceeds via a transition-state structure lying 0.7 kcal/mol below the energy of reactants at 0 K, whereas the HO• addition to the central carbon atom takes place via a transition-state structure lying 0.8 kcal/mol above the energy of the reactants at 0 K. On the basis of conventional transition-state theory calculations at 298 K, it is predicted that 74.5% of the HO• reaction with acrolein proceeds via abstraction of the aldehydic H-atom, 24.2% via HO• addition to the terminal carbon atom of the double bond, and 1.3% via HO• addition to the central carbon atom of the double bond. These results are in close agreement with available experimental data.

1. Introduction

Acrolein (CH_2═CH-CHO) is an unsaturated aldehyde present in the atmosphere as the result of direct anthropogenic emissions (e.g., from combustion sources) or as the result of the atmospheric hydroxyl radical (HO•)- and ozone (O_3)-initiated oxidation of 1,3-dienes.[1–4] In several large cities, ambient concentrations up to 9 ppb of acrolein have been reported.[5] Similarly to other unsaturated carbonyl compounds, the main degradation process of acrolein under atmospheric conditions is via reaction with HO•, with photolysis and reaction with O_3 and nitrate radical (NO_3•) playing at most a minor role.

The reported rate constants for HO• reaction with acrolein[6–10] are in the range $(1.83-2.66) \times 10^{-11}$ cm^3 molecule^{-1} s^{-1}, and only three product studies on this reaction have been published so far.[10–12] Magneron et al.[10] published data which suggested that ≈20−25% of the reaction of HO• with acrolein occurs via addition to the C═C double bond. In a subsequent work, Orlando and Tyndall[12] determined that about 68% of the HO• reaction with acrolein proceeds via abstraction of the aldehydic H-atom (i.e., reaction of eq 1), with the remainder occurring via addition to the C═C double bond (i.e., reactions of eqs 2 and 3). These results are in moderate

$$CH_2=CHCHO + HO\cdot \rightarrow CH_2=CHC\cdot O + H_2O \quad (1)$$

$$CH_2=CHCHO + HO\cdot \rightarrow HOCH_2C\cdot HCHO \quad (2)$$

$$CH_2=CHCHO + HO\cdot \rightarrow \cdot CH_2CH(OH)CHO \quad (3)$$

agreement with those of the study by Magneron et al.[10] An additional unresolved question concerns the actual site of the HO• addition (i.e., on the terminal carbon atom (reaction

* Corresponding author e-mail: sonqtc@iiqab.csic.es.
† Institut d'Investigacions Químiques i Ambientals de Barcelona.
‡ Universitat de Barcelona.

10.1021/ct8000798 CCC: $40.75
Published on Web 05/21/2008

of eq 2) or on the central carbon atom (reaction of eq 3)). On the basis of their product study, Orlando and Tyndall[12] estimated that at least 80% of the HO• addition takes place on the terminal carbon atom.

We feel that the results of the experimental studies of Magneron et al.[10] and Orlando and Tyndall[12] merit a theoretical study to analyze the subtle balance between the different pathways in the HO• reaction with acrolein. With this aim, herein we report the results of high level quantum-mechanical electronic structure calculations on the low-energy reaction pathways of eqs 1–3[13] The energetic, structural, and vibrational results furnished by these calculations are subsequently used to perform conventional transition-state computations to predict the rate coefficients and the branching ratios of the competing addition and abstraction reactions.

2. Computational Details

2.1. Electronic Structure Calculations. The geometries of the relevant stationary points (minima and first-order saddle points) on the lowest-energy potential energy surface (PES) of each reaction system were optimized by using the spin-unrestricted quadratic configuration-interaction method with all single and double excitations,[15] denoted as UQCISD, with core−electrons excluded (frozen core approximation), employing Dunning's augmented correlation-consistent polarized valence double-ζ (aug-cc-pVDZ) basis set.[16] The harmonic vibrational frequencies of these stationary points were computed at the latter level of theory. Connections of the transition-state structures between designated minima were confirmed in each case by intrinsic reaction coordinate (IRC)[17] calculations using the second-order algorithm of Gonzalez and Schlegel.[18]

Since energy barriers affect the calculated rate coefficients exponentially, it is crucial to compute accurately the energies of the transition-state structures relative to those of the reactants. A special difficulty is encountered in the case of the transition-state structures located for the competing reactions of eqs 1–3 because we found a significant difference in the degree of "spin contamination" shown by the spin-unrestricted Hartree−Fock (UHF) wave function underlying the UQCISD calculations. In fact, the expected values of the spin-squared operator S^2 for the UHF/aug-cc-pVDZ wave function of the transition-state structures calculated for these reactions were found to be 0.7654, 1.0952, and 1.0815, respectively. Therefore, all the energies were refined by performing single point energy calculations on the UQCISD geometries using the (frozen core) UQCISD method with a perturbative estimation of all connected triple excitations,[15] denoted as UQCISD(T). Finally, energies were also evaluated from partially spin-adapted QCISD(T) calculations based on a restricted open-shell Hartree−Fock reference determinant,[19] denoted as RQCISD(T), to accomplish the spin contamination in spin-unrestricted quadratic configuration-interaction wave functions.[20] The related spin-restricted coupled-cluster method[21] including all single and double excitations with a perturbative estimation of all connected triple excitations,[22] denoted as RCCSD(T), has been shown[23] to achieve "chemical accuracy" even in situations where spin contamination would normally be a problem. However, Senosiain et al.[14,24] have recently concluded that the RQCISD(T) method performs slightly better than RCCSD(T) in the calculation of a series of well-known adiabatic energy barriers.[25] Both the UQCISD(T) and RQCISD(T) calculations were carried out with Dunning's augmented correlation-consistent polarized valence triple-ζ (aug-cc-pVTZ) basis set.[16]

Zero-point vibrational energies (ZPVEs) were determined from unscaled harmonic vibrational frequencies. Thermal corrections to enthalpy and Gibbs energy values were obtained assuming ideal gas behavior from the unscaled harmonic frequencies and moments of inertia by conventional methods.[26] A standard pressure of 1 atm was taken in the absolute entropies calculations.

For the hydrogen-bonded complexes found in this work, the basis set superposition error (BSSE) was calculated at the UQCISD(T)/aug-cc-pVTZ level by using the counterpoise method of Boys and Bernardi.[27]

To examine the characteristics of the bonding and interactions in the most relevant structures we have also performed an analysis of the electron density within the framework of the topological theory of atom in molecules (AIM).[28] The net atomic charges were examined by means of the Mulliken population analysis.[29] The Z density matrix obtained from UQCISD gradient calculations with the aug-cc-pVDZ basis set, an effective correlated density matrix,[30] was used in both analyses.

All the UQCISD and UQCISD(T) calculations were carried out by using the Gaussian 03 program package,[31] whereas the MOLPRO 98 program package[32] was employed for the RQCISD(T) computations. The PROAIM and EXTREME programs of Bader et al.[33] were used to perform the AIM analysis of the electronic density.

2.2. Rate Coefficient Calculations. With the main purpose of evaluating the overall rate coefficient of the HO• reaction with acrolein, conventional transition-state theory calculations were carried out for reactions of eqs 1–3. As it will be shown in section 4, all these reaction pathways consist of a reversible first step involving the barrierless formation of a prereaction loosely bound complex in the entrance channel, followed by the irreversible formation of products. Therefore, each reaction pathway is a two-step process as described by eq 4, where the corresponding complex is in equilibrium with the reactants

$$CH_2=CHCHO^{\bullet} + HO \underset{k_{-1}}{\overset{k_1}{\rightleftharpoons}} \text{Complex} \xrightarrow{k_2} \text{Products} \qquad (4)$$

If k_1 and k_{-1} are the rate constants for the first step and k_2 is the rate constant for the second step, then a steady-state analysis leads[34] to an overall rate constant for the reaction pathway under consideration, denoted as k_{RP}, which can be approximated as

$$k_{RP} = \frac{k_1}{k_{-1}} k_2 = K_{eq} k_2 \qquad (5)$$

where K_{eq} stands for the equilibrium constant in the first step, which can be written as

$$K_{eq} = \frac{Q_{CX}}{Q_{CH2=CHCHO} Q_{HO}} e^{\frac{-(E_C - E_R)}{RT}} \quad (6)$$

where the various Qs are the partition functions of the reactants ($Q_{CH2=CHCHO}$ and Q_{HO}) and prereaction complex (Q_{CX}); E_R and E_{CX} are the total electronic energy plus the ZPVE of the reactants and prereaction complex, respectively; R is the ideal gas constant; and T is the absolute temperature. The rate constant k_2 can be evaluated using the conventional transition-state theory equation[35]

$$k_2 = \Gamma \frac{k_b T}{h} \frac{Q_{TS}}{Q_{CX}} e^{\frac{-(E_{TS} - E_{CX})}{RT}} \quad (7)$$

where Q_{TS} and E_{TS} are the partition function and the total electronic energy plus ZPVE, respectively, of the transition state, and Γ is the tunneling factor.

According to the standard formulas,[26] the Qs were evaluated using the UQCISD/aug-cc-pVDZ geometries and harmonic vibrational frequencies, while the Es were taken as the ZPVE-corrected QCISD(T)/aug-cc-pVTZ energies. The Γs were evaluated by zero-order approximation to the vibrationally adiabatic PES model with zero curvature.[36] In this approximation the tunneling is assumed to occur along a unidimensional minimum energy path. The potential energy curve is approximated by an unsymmetrical Eckart potential energy barrier[37] that is required to go through the ZPVE corrected energy (denoted as E) of the reactants, transition state, and products. The equations that describe the Eckart potential energy function were adapted from Truong and Truhlar.[36] Solving the Schroedinger equation for the Eckart function yields the transmission probability, $\kappa(E)$. Then Γ is obtained by integrating the respective $\kappa(E)$ over all possible energies:

$$\Gamma(T) = \frac{1}{k_b T} e^{\frac{E_{TS} - E_{CX}}{RT}} \int_0^\infty e^{\frac{-E_{TS}}{RT}} \kappa(E) dE \quad (8)$$

3. Preliminary Test for the Aldehydic H-Atom Abstraction from Acetaldehyde by an HO Radical

To confirm the reliability of the theoretical methods described above in predicting the rate coefficient for H-atom abstraction from aldehydes by hydroxyl radicals, we tested these methods on the reaction of acetaldehyde (CH_3CHO) with HO$^\bullet$ (eq 9).

$$CH_3CHO + HO^\bullet \rightarrow CH_3C^\bullet O + H_2O \quad (9)$$

Previous theoretical work on the reaction of eq 9 by Vivier-Bunge et al.,[38] using geometries optimized at the UMP2 level with the 6−311++G(d,p) basis set[39] and single point energy calculations at the UCCSD(T) level employing the same basis set, has shown that the reaction is not elemental. It consists of a reversible first step involving the formation of a prereaction hydrogen-bonded complex, followed by the irreversible formation of a loosely bound complex between the products $CH_3C^\bullet O$ and H_2O. Selected geometrical parameters of the prereaction hydrogen-bonded complex (labeled as **CXR**), transition-state structure (labeled as **TS**), and the loosely bound complex between the products

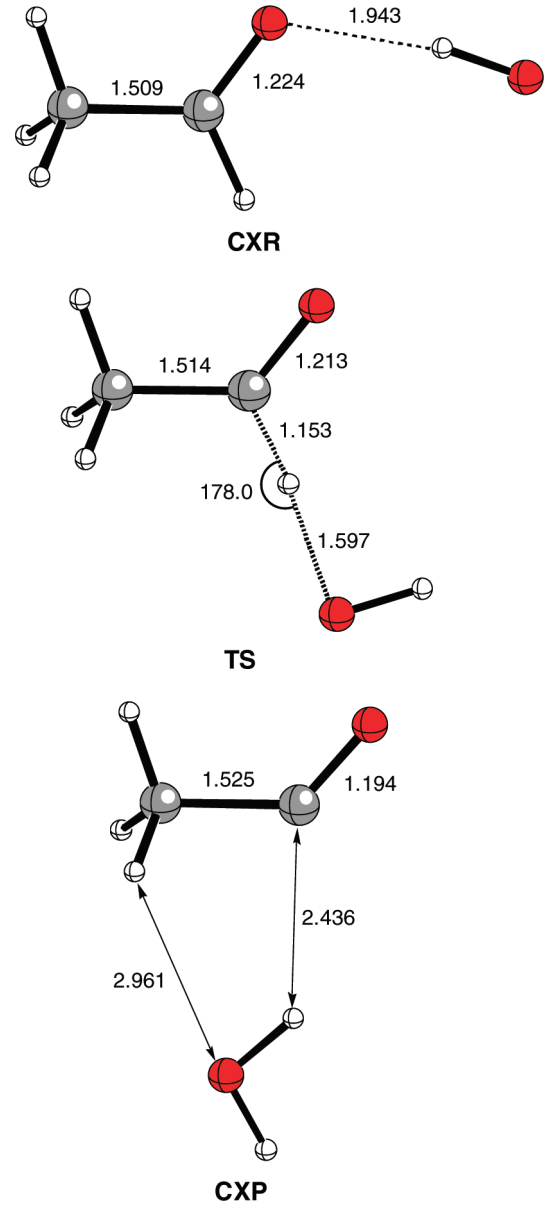

Figure 1. Selected geometrical parameters of the most relevant structures of the reaction pathway for the aldehydic H-atom abstraction from acetaldehyde by HO$^\bullet$. Distances are given in Å and angles in deg.

(labeled as **CXP**) calculated at the UQCISD/aug-cc-pVDZ level for the reaction of eq 9 are shown in Figure 1. The Cartesian coordinates of all structures reported in this article are available as Supporting Information. Total electronic energies computed at the different levels of theory as well as the ZPVEs, thermal corrections to enthalpy and Gibbs energy, for the structures concerning the reaction of eq 9 are collected in Table S1 (Supporting Information). Table 1 gives the relative electronic energies (designated by ΔU) as well as the relative energies at 0 K (designated by ΔE(0 K)) and the relative enthalpies (designated by ΔH(298 K)) and Gibbs energies (designated by ΔG(298 K)) at 298 K, for these structures calculated at both the UQCISD(T) and RQCISD(T) levels of theory with the aug-cc-pVTZ basis set. The equilibrium constant (K_{eq}) of the first step, the tunneling factor (Γ) and the rate coefficient (k_2) of the second

Table 1. Relative Energies (kcal/mol) of the Most Relevant Stationary Points on the Ground-State Potential Energy Surface for the Aldehydic H-Atom Abstraction from Acetaldehyde by HO•[a]

stationary point[b]	ΔU	ΔE (0 K)	ΔH (298 K)	ΔG (298 K)
$CH_3CHO + HO^•$	0.0	0.0	0.0	0.0
CXR	−6.1 (−6.1)	−4.0 (−4.0)	−4.7 (−4.7)	2.1 (2.1)
TS	−1.2 (−1.7)	−1.1 (−1.6)	−1.7 (−2.2)	5.7 (5.2)
CXP	−32.7 (−32.9)	−31.0 (−31.2)	−30.6 (−30.8)	−25.5 (−25.7)
$CH_3CO^• + H_2O$	−29.3 (−29.2)	−29.0 (−28.9)	−28.6 (−28.5)	−29.8 (−29.7)

[a] Calculated at the RQCISD(T) level of theory with the aug-cc-pVTZ basis set. The values calculated at the UQCISD(T) level with the same basis set are given in parentheses. [b] See Figure 1.

Table 2. Equilibrium Constant (K_{eq} in molecule^{-1} cm^3; See Eq *6*) of the First Step, Tunneling Factor (Γ) and Rate Coefficient (k_2 in molecule^{-1} cm^3 s^{-1}; See Eq *7*) of the Second Step, and Overall Rate Coefficient (k_{RP} in molecule^{-1} cm^3 s^{-1}; See Eq *5*) at 298 K of the Reaction Pathway for the Aldehydic H-Atom Abstraction from Acetaldehyde by HO•

method	K_{eq}	Γ	k_2	k_{RP}
UQCISD(T)	1.1894×10^{-21}	1.0300	3.2768×10^{10}	3.8974×10^{-11}
RQCISD(T)	1.1894×10^{-21}	1.0320	1.4119×10^{10}	1.6793×10^{-11}
exp[a]				1.6×10^{-11}

[a] Reference 38.

step, and the overall rate coefficient (k_{RP}) at 298 K for the reaction of eq 9 are summarized in Table 2.

The geometries calculated for **CXR**, **TS**, and **CXP** (Figure 1) compare well with those computed at the UMP2 level with the 6−311++G(d,p) basis set by Vivier-Bunge et al.[38] However, on the basis of the bond lengths of the breaking C−H and forming H−O bonds in **TS**, it turns out that the present UQCISD/aug-cc-pVDZ calculations predict a transition-state structure which is somewhat more reactant-like than that calculated at the UMP2/6−311++G(d,p) level. The activation energy at 0 K (designated by $\Delta E^‡$(0 K)) of −1.6 kcal/mol calculated at the UQCISD(T)/aug-cc-pVTZ+ZPVE level (see Table 1) is in good agreement with the $\Delta E^‡$(0 K) of −1.71 kcal/mol obtained by Vivier-Bunge et al.[38] from UCCSD(T)/6−311++G(d,p)+ZPVE calculations, whereas the $\Delta E^‡$(0 K) of −1.1 kcal/mol computed at the RQCISD(T)/aug-cc-pVTZ+ZPVE level is 0.6 kcal/mol higher than the latter value. Nevertheless, the energy barrier (designated by $\Delta U^‡$) of −1.2 kcal/mol evaluated from the RQCISD(T) calculations (see Table 1) leads to an the overall rate coefficient at 298 K of 1.6793×10^{-11} molecule^{-1} cm^3 s^{-1} (see Table 2), which is in excellent agreement with the experimental[40] value of 1.6×10^{-11} molecule^{-1} cm^3 s^{-1}. In contrast, the $\Delta U^‡$ of −1.7 kcal/mol calculated at the UQCISD(T) level leads to an overall rate coefficient at 298 K of 3.8974×10^{-11} molecule^{-1} cm^3 s^{-1}, which is too large by a factor of 2.4 as compared to the experimental result. Therefore, it appears that the RQCISD(T) method performs better than UQCISD(T) in the calculation of the rate coefficient for H-atom abstraction from aldehydes by hydroxyl radicals, This finding may be partially explained by the fact that spin contamination is eliminated in the RQCISD(T) calculation of the energy barrier.

4. Results and Discussion

Figure 2 displays a schematic energy profile showing the most relevant structures concerning the main pathways on the lowest-energy PES for the reaction of HO• with acrolein. Figures 3 and 4 show selected geometrical parameters, and Table 3 gives the values of ΔU, ΔE(0 K), ΔH(298 K), and ΔG(298 K) calculated for these structures. Their total electronic energies computed at the different levels of theory as well as the ZPVEs, thermal corrections to enthalpy and Gibbs energy, are collected in Table S1 (Supporting Information). Finally, the values of K_{eq}, Γ, k_2, and the overall rate coefficient (k_{RP}) at 298 K for reactions of eqs 1–3 are summarized in Table 4.

4.1. Aldehydic H-Atom Abstraction from Acrolein by HO Radical. Two conformers for acrolein exist, due to internal rotation around the C−C single bond joining the vinyl and the aldehyde moieties of the molecule. Depending on whether the C═O and the C═C double bonds appear on the same or opposite side with respect to the C−C single bond, the conformer is called synperiplanar (labeled as **1-sp**) or antiperiplanar (labeled as **1-ap**). The QCISD/aug-cc-pVDZ minimum-energy structures corresponding to these two conformomers are shown in Figure S1 (Supporting Information). At the QCISD(T)/aug-cc-pVTZ level the **1-ap** conformer turns out to be 1.83 kcal/mol more stable than the **1-sp** conformer in terms of Gibbs energy at 298 K. This result provides an equilibrium constant $K_p°$ of 0.045, which gives an **1-ap**:1-**sp** population ratio of 95.66:4.34. Thus, it seems that just the **1-ap** conformer of acrolein has significant weight in its reactivity at room temperature. Therefore, we have only taken into account the reactions of HO• with the **1-ap** conformer.

As for acetaldehyde and in many gas-phase reactions of interest in atmospheric chemistry, Figure 2 shows that the aldehydic H-atom abstraction from acrolein by HO• begins with the barrierless formation of a prereaction complex in the entrance channel. The optimized geometry of this complex, labeled as **CXR1** (Figure 3), has C_s symmetry and was characterized as a true local minimum on the PES. The AIM topological analysis of the electron density in **CXR1** revealed the presence of a bond critical point between the oxygen atom of acrolein and the hydrogen atom of HO•, indicating that there is a bonding interaction between these atom pairs. The low value of the electron density (0.0262 e bohr^{-3}), the positive value of the its Laplacian (0.0892 e bohr^{-5}), and the positive value of the local energy density[41]

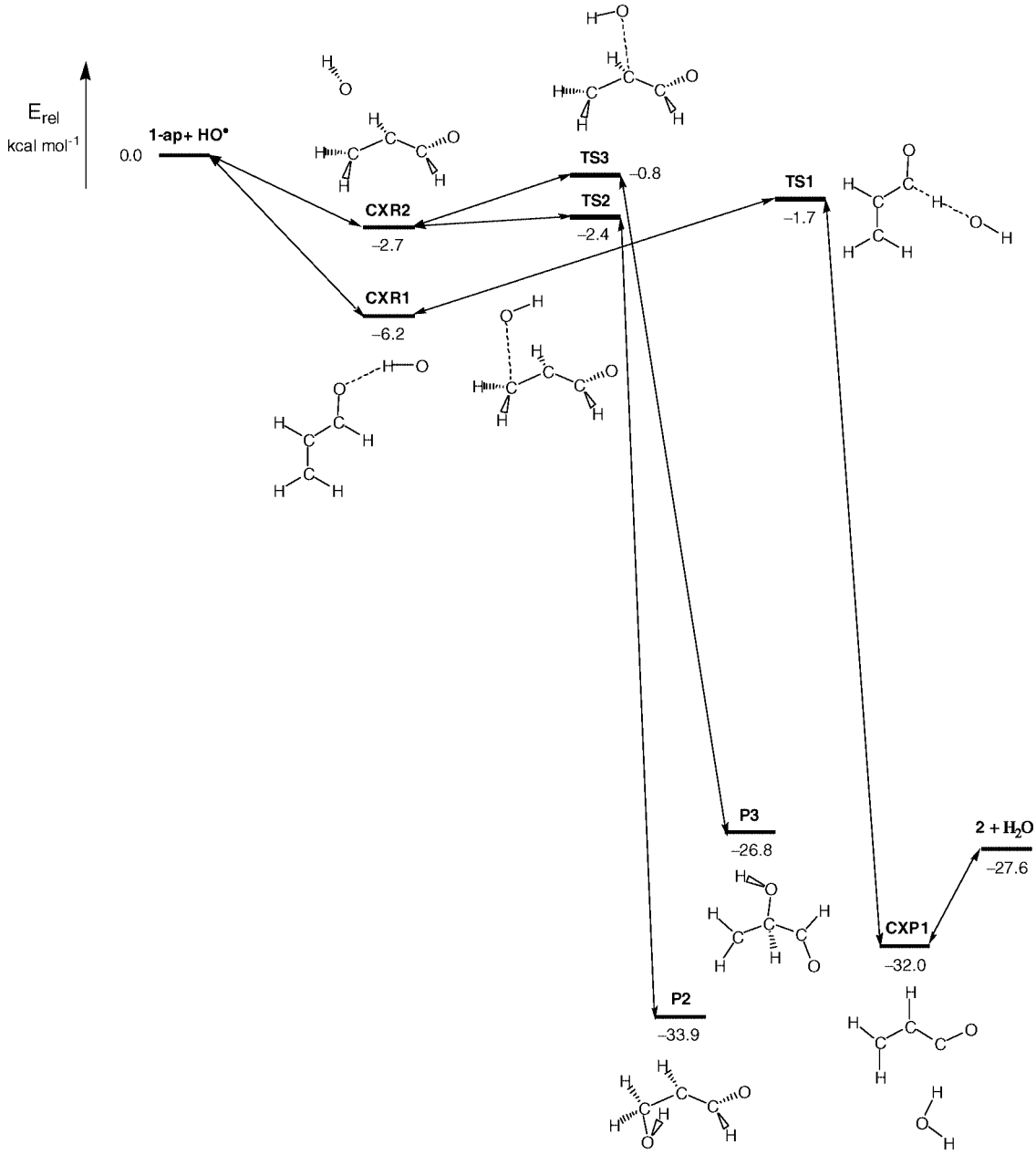

Figure 2. Schematic energy profiles showing the most relevant structures of the reaction pathways on the ground-state potential energy surface for the reaction of HO• with acrolein. Relative energy values calculated at the RQCISD(T) level of theory with the aug-cc-pVTZ basis set.

(0.0011 hartree bohr^{-3}) calculated for this bond critical point is typically associated with hydrogen-bond-like interactions. Therefore, it turns out that **CXR1** is a hydrogen-bonded complex.

The hydrogen-bond distance in **CXR1** is nearly identical to that calculated for the prereaction hydrogen-bonded complex **CXR** found in the H-atom abstraction of acetaldehyde (see Figure 1). In addition, the calculated ΔU (see Tables 1 and 3) indicate that **CXR1** and **CXR** lie 6.2 and 6.1 kcal/mol, respectively, below the energy of the isolated reactants. Therefore, the stabilization energy of these hydrogen-bonded complexes is also nearly identical. Inclusion of the correction for the BSSE leads to a stabilization energy of **CXR1** toward decomposition into their components of 5.7 kcal/mol.

After forming the prereaction hydrogen-bonded complex **CXR1**, the aldehydic H-atom is transferred from the acrolein to the HO• moiety through the transition-state structure labeled as **TS1**, displayed in Figure 3, which has C_s symmetry. A comparison between the geometries calculated for **TS1** and **TS** reveals that the bond lengths of the breaking C−H and forming H−O bonds as well as the C−H−O bond angle of both transition-state structures are very similar. The ΔU data listed in Table 3 show that **TS1** lies 1.7 kcal/mol below the energy of the reactants and 4.5 kcal/mol above the energy of **CXR1**. Inclusion of ZPVE corrections to energy leads to a $\Delta E^{\ddagger}$(0 K) of −1.1 kcal/mol for the aldehydic H-atom abstraction from acrolein by HO•. This value is identical to the $\Delta E^{\ddagger}$(0 K) calculated for acetaldehyde (see Table 1). However, the ΔG(298 K) data listed in Tables

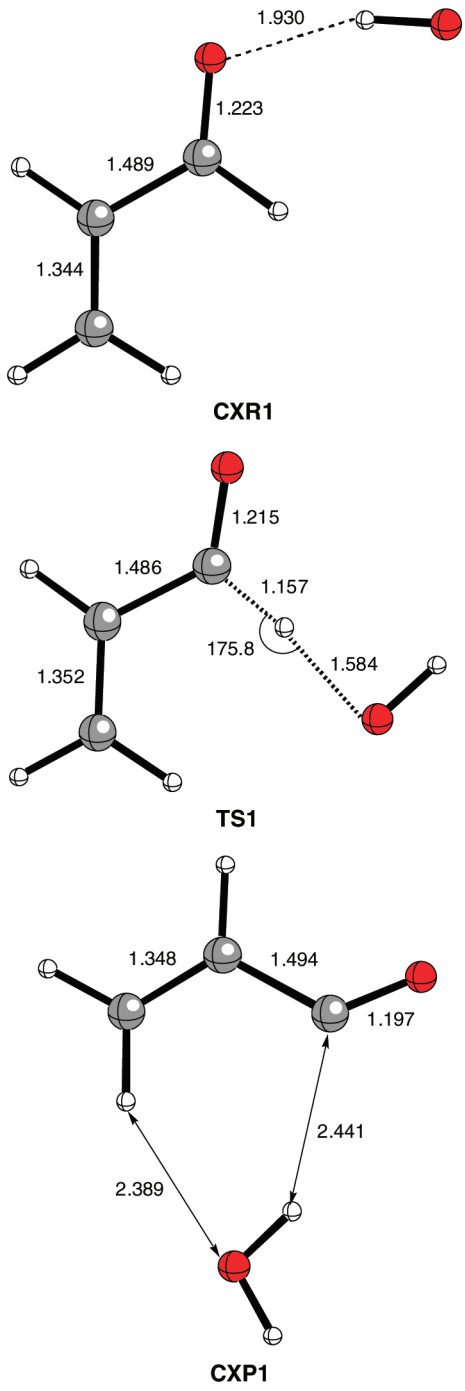

Figure 3. Selected geometrical parameters of the most relevant structures of the reaction pathway for the aldehydic H-atom abstraction from acrolein by HO•. Distances are given in Å and angles in deg.

1 and 3 show that the Gibbs energies of activation at 298 K (designated by $\Delta G^{\ddagger}$(298 K)) for the aldehydic H-atom abstraction from acrolein and acetaldehyde by HO• are calculated to be 6.3 and 5.7 kcal/mol, respectively.

The IRC calculations showed that **TS1** goes backward to **CXR1** and goes forward to give a product complex in which the already formed water is loosely bound to the CH_2═CHCO radical fragment. The optimized geometry of this complex, labeled as **CXP1** (Figure 3), was characterized as a true local minimum on the PES. The ΔU data listed in Table 3 show that **CXP1** lies 4.4 kcal/mol below the energy of the isolated products H_2O and CH_2═CHC•O (designated by **2**). Inclusion of the correction for the BSSE leads to a stabilization energy of **CXP1** toward decomposition into H_2O and **2** of 3.9 kcal/mol. We did not find an energetic barrier other than that imposed by the endoergicity for the **CXP1** complex to break apart to form the latter products. At this point we note that the aldehydic H-atom abstraction from acrolein by HO• is predicted to be exoergic. Thus, according to Table 3 the energy of reaction at 0 K (designated by ΔE_r(0 K)) is calculated to be −27.1 kcal/mol. This exoergicity is 1.9 kcal/mol lower than that calculated for acetaldehyde (see Table 1).

Concerning the results of the conventional transition-state theory calculations for the reaction of eq 1 given in Table 4, first we note that the value of 1.0345 calculated for the tunneling factor Γ indicates that the tunneling effect in the reaction of eq 1 is negligible. This feature is contrary to common belief that for an H-atom transfer process the tunneling effect should be important. However, it is worth noticing that for the related reaction of eq 9 the tunneling effect is also unimportant because the value of Γ is calculated to be 1.0320 (see Table 2). These unexpected results are ascribed to the fact that the energy barriers of reactions of eqs 1 and 9 are broad, as suggested by the small value of the imaginary vibrational frequency of the corresponding transition-state structure. Thus, the imaginary frequencies calculated at the UQCISD/aug-cc-pVDZ level for **TS** and **TS1** were found to be 207.9*i* and 221.9*i* cm^{-1}, respectively. Second, we note that the rate coefficient at 298 K of 5.7590 × 10^{-12} $molecule^{-1}$ cm^{-3} s^{-1} predicted for the reaction of eq 1 is about 1 order of magnitude smaller than the value of 1.6793 × 10^{-11} $molecule^{-1}$ cm^{-3} s^{-1} calculated for the reaction of eq 9 (see Tables 2 and 4). Since in both reactions the tunneling effect is negligible, these results may be partially explained by the fact that the $\Delta G^{\ddagger}$(298 K) calculated for the aldehydic H-atom abstraction from acrolein (6.3 kcal/mol) is 0.6 kcal/mol higher than that calculated for acetaldehyde (5.7 kcal/mol).

4.2. HO• Addition to the Acroleine C═C Double Bond. As for the aldehydic H-atom abstraction, the HO• addition to the C═C double bond of acrolein begins with the barrierless formation of a prereaction complex in the entrance channel (see Figure 2). The optimized geometry of this complex, labeled as **CXR2** (Figure 4), was characterized as a true local minimum on the PES. The net atomic charges evaluated by using the Mulliken population analysis of the effective UQCISD/aug-cc-pVDZ electron density showed an electron charge transfer in **CXR2** of 0.004 e in the direction acrolein → HO• due to a weak delocalization of the π electron density of the C═C double bond into the antibonding σ^*(HO) orbital of the HO•. This result indicates that the dominant attractive interactions holding in association the acrolein and HO• partners in the **CXR2** complex arise mainly from dispersion forces. Therefore, **CXR2** is a van der Waals loosely bound complex.

As shown in Figure 4, the distance between the oxygen atom of the HO• moiety and the C═C double bond carbon atoms of the acrolein moiety are very long (i.e., 2.830 and 2.934 Å). Therefore, the structural perturbation of the two

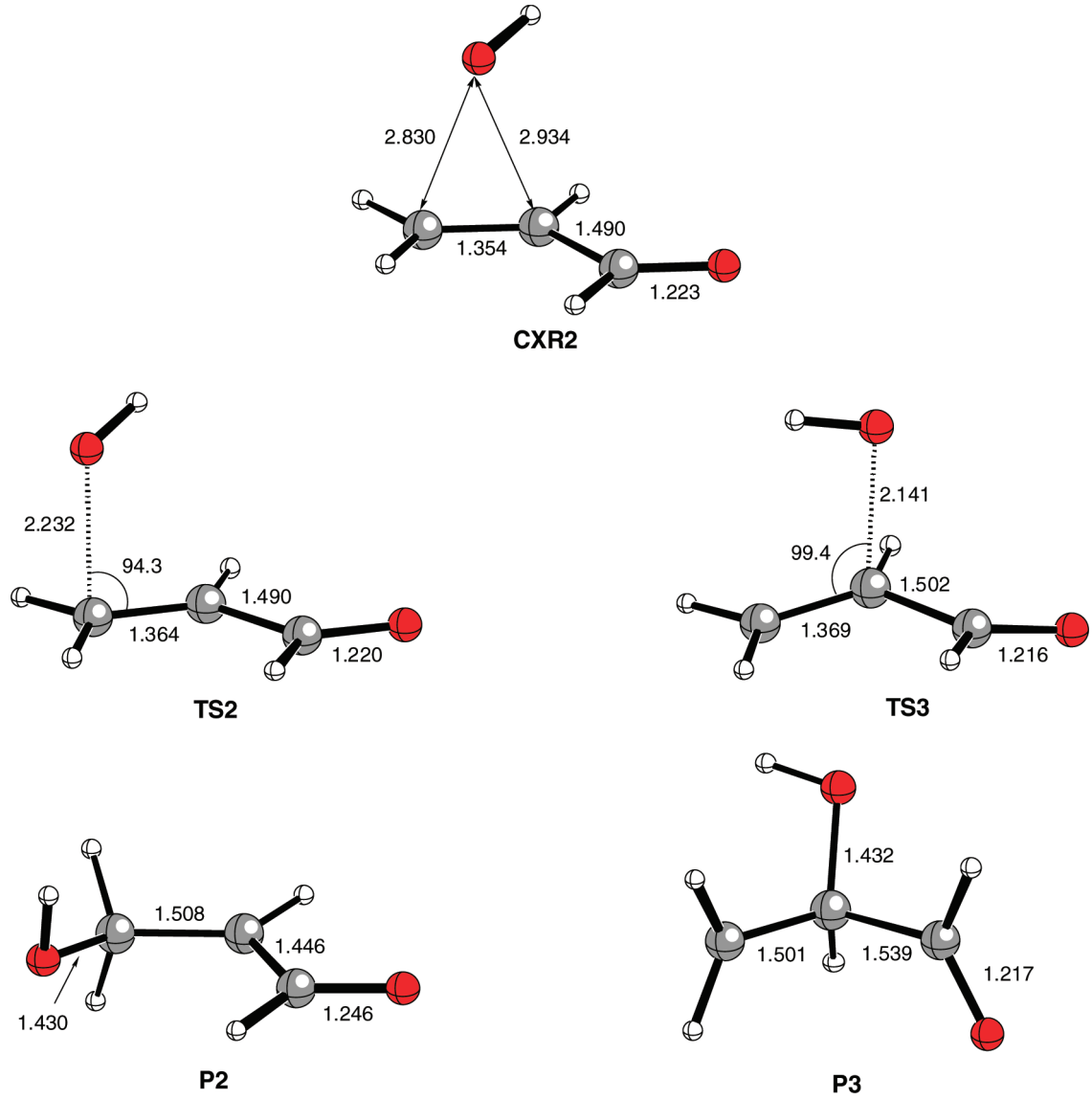

Figure 4. Selected geometrical parameters of the most relevant structures of the reaction pathway for the HO• addition to the C═C double bond of acrolein. Distances are given in Å and angles in deg.

Table 3. Relative Energies (kcal/mol) of the Most Relevant Stationary Points on the Ground-State Potential Energy Surface for the Aldehydic H-Atom Abstraction by HO• and the HO• Addition to the C═C Double Bond of Acrolein[a]

stationary point[b]	ΔU	ΔE (0 K)	ΔH (298 K)	ΔG (298 K)
1-ap + HO•	0.0	0.0	0.0	0.0
CXR1	−6.2	−4.0	−4.4	2.9
TS1	−1.7	−1.1	−1.8	6.3
CXP1	−32.0	−30.0	−29.7	−23.7
2 + H_2O	−27.6	−27.1	−26.8	−27.9
CXR2	−2.7	−1.7	−1.6	4.7
TS2	−2.4	−0.7	−1.5	7.1
TS3	−0.8	0.8	0.0	8.8
P2	−33.9	−29.7	−30.8	−21.3
P3	−26.8	−23.8	−24.7	−15.4

[a] Calculated at the RQCISD(T) level of theory with the aug-cc-pVTZ basis set. [b] See Figure 2.

partners in the **CXR2** complex is insignificant as compared with the separated species. The calculated ΔU (see Table 3) indicate that **CXR2** lies 2.7 kcal/mol below the energy of the isolated reactants. Inclusion of the correction for the BSSE leads to a stabilization energy of **CXR2** toward decomposition into their components of 2.1 kcal/mol.

After forming the prereaction complex **CXR2**, the reaction bifurcates into two different pathways. The lowest-energy barrier reaction pathway is the addition of HO• to the terminal carbon atom of the C═C double bond through the transition-state structure labeled as **TS2**, displayed in Figure 4. **TS2** shows a conserved character of the C═C double bond, planarity of the π system, and a long distance between the carbon and oxygen atoms (2.232 Å). Therefore, **TS2** is a reactant-like transition-state structure. The ΔU data listed in Table 3 show that **TS2** lies 2.4 kcal/mol below the energy of the reactants and 0.3 kcal/mol above the energy of **CXR2**. Inclusion of ZPVE corrections to energy leads to a $\Delta E^{\ddagger}$(0 K) of −0.7 kcal/mol for the HO• addition to the terminal carbon atom of the C═C double bond of acrolein. This value is 0.4 kcal/mol higher than the $\Delta E^{\ddagger}$(0 K) calculated for the aldehydic H-atom abstraction by HO•. However, the ΔG(298 K) data listed in Table 3 show that the $\Delta G^{\ddagger}$(298 K) for the HO• addition to the terminal carbon atom of the C═C double

Table 4. Equilibrium Constant (K_{eq} in molecule^{-1} cm^3; See Eq *6*) of the First Step, Tunneling Factor (Γ) and Rate Coefficient (k_2 in molecule^{-1} cm^3 s^{-1}; See Eq *7*) of the Second Step, and Rate Coefficient (k_{RP} in molecule^{-1} cm^3 s^{-1}; See Eq *5*) at 298 K of the Reaction Pathways for the Aldehydic H-Atom Abstraction by HO$^\bullet$ and the HO$^\bullet$ Addition to the C=C Double bond of Acrolein

reaction pathway	K_{eq}	Γ	k_2	k_{RP}
reaction eq 1	2.8906×10^{-22}	1.0345	1.9923×10^{10}	5.7590×10^{-12}
reaction eq 2	1.4950×10^{-23}	1.1229	1.2534×10^{11}	1.8739×10^{-12}
reaction eq 3	1.4950×10^{-23}	1.1013	6.5421×10^{9}	9.7535×10^{-14}
all[a]				0.77304×10^{-11}
exp[b]				2.0×10^{-11}

[a] Sum of the k_{RP} calculated for the three reaction pathways. [b] Reference 10.

bond of acrolein is 0.8 kcal/mol higher than the $\Delta G^{\ddagger}$(298 K) calculated for the aldehydic H-atom abstraction by HO$^\bullet$.

The IRC calculations showed that **TS2** goes backward to **CXR2** and goes forward to give the reaction product of reaction of eq 2. The optimized geometry of this adduct, labeled as **P2** (Figure 4), was characterized as a true local minimum on the PES. According to Table 3, the ΔE_r(0 K) for the reaction of eq 2 is calculated to be −29.7 kcal/mol. This exoergicity is 2.6 kcal/mol larger than that calculated for the reaction of eq 1.

As can be observed in Figure 2, the addition of HO$^\bullet$ to the central carbon atom of the C=C double bond takes place through the transition-state structure labeled as **TS3**, displayed in Figure 4. Like as found for **TS2**, the geometries of the reactants are only slightly perturbed in **TS3**, preserving the planarity of the C=C double bond π system. The distance between the carbon and oxygen atoms is long (2.141 Å). Therefore, **TS3** is also a reactant-like transition-state structure. The ΔU data listed in Table 3 show that **TS3** lies 0.8 kcal/mol below the energy of the reactants and 1.9 kcal/mol above the energy of **CXR2**. Inclusion of ZPVE corrections to energy leads to a $\Delta E^{\ddagger}$(0 K) of 0.8 kcal/mol for the HO$^\bullet$ addition to the central carbon atom of the C=C double bond. This value is 1.5 kcal/mol higher than the $\Delta E^{\ddagger}$(0 K) calculated for the for the HO$^\bullet$ addition to the terminal carbon atom of the C=C double bond.

The IRC calculations showed that **TS3** goes backward to **CXR2** and goes forward to give the reaction product of reaction of eq 3. The optimized geometry of this adduct, labeled as **P3** (Figure 4), was characterized as a true local minimum on the PES. According to Table 3, the ΔE_r(0 K) for the reaction of eq 3 is calculated to be −23.8 kcal/mol. This exoergicity is 5.9 kcal/mol lower than that calculated for the reaction of eq 2.

Our calculations show that the HO$^\bullet$ addition to the C=C double bond of acrolein is a very regioselective reaction. In fact, the difference of 1.7 kcal/mol between the $\Delta G^{\ddagger}$(298 K) calculated for reactions of eqs 2 and 3 (see Table 3) clearly indicates that HO$^\bullet$ attacks preferentially the less substituted carbon atom of the C=C double bond. Furthermore, on comparing the calculated overall rate coefficients in Table 4, it can be seen that at 298 K the HO$^\bullet$ addition to the terminal carbon atom of the C=C double bond is about 19 times faster than the addition to the central carbon atom. Specifically, the overall rate coefficients at 298 K calculated for reactions of eqs 2 and 3 lead to a branching ratio of 95.1:4.9, which is in good agreement with experimental data indicating that at least 80% of the HO$^\bullet$ addition takes place on the terminal carbon atom.[12]

The overall rate coefficients at 298 K listed in Table 4 show that the rate coefficient predicted for the reaction of eq 1 (0.57590×10^{-11} molecule^{-1} cm^{-3} s^{-1}) is about 3 times as large as that of the reaction of eq 2 (0.18739×10^{-11} molecule^{-1} cm^{-3} s^{-1}) and about 59 times larger than that of reaction of eq 3 (0.00975×10^{-11} molecule^{-1} cm^{-3} s^{-1}). As a consequence, the sum of the rate coefficients at 298 K calculated for the reactions of eqs 1 and 2 (i.e., 0.76329×10^{-11} molecule^{-1} cm^{-3} s^{-1}) is nearly identical to the value (0.77304×10^{-11} molecule^{-1} cm^{-3} s^{-1}) of the global rate coefficient at 298 K estimated for the reaction of HO$^\bullet$ with acrolein (see Table 4). At this point it is worth noting that the latter value is roughly in reasonable agreement with the reported experimental rate coefficients[6–10] ranging from 1.83 to 2.66×10^{-11} cm^3 molecule^{-1} s^{-1}. Furthermore, the overall rate coefficients at 298 K calculated for reactions of eqs 1–3 lead to a branching ratio of 74.5:24.2:1.3, which is in good agreement with experimental data indicating that about 68% of the HO$^\bullet$ reaction with acrolein proceeds via abstraction of the aldehydic H-atom, with the remainder occurring via addition to the C=C double bond.[12]

5. Summary and Conclusions

High level quantum-mechanical electronic structure calculations (UQCISD and RQCISD(T)) were carried out to analyze the subtle balance between the different pathways involved in the HO$^\bullet$ reaction with acrolein under atmospheric conditions. The energetic, structural, and vibrational results furnished by these calculations were subsequently used to perform conventional transition-state computations to predict the rate coefficients and the branching ratios of the competing abstraction and addition reactions. From the analysis of the results, the following main points emerge.

(1) The first step of all the reaction pathways studied involves the barrierless formation of a prereaction loosely bound complex in the entrance channel, lying a few kcal/mol below the energy of the reactants.

(2) The lowest-energy barrier pathway at 0 K is found to be the abstraction of the aldehydic H-atom through a transition-state structure lying 1.1 kcal/mol below the energy of the reactants. A tunneling factor of 1.0345 at 298 K is calculated for this H-atom transfer reaction. On the basis of the small value of the imaginary frequency calculated for the transition-state structure, this unexpected result is ascribed to the broad energy barrier of the reaction.

(3) After forming the prereaction complex in the HO• addition entrance channel, the reaction bifurcates into two different pathways. The lowest-energy barrier pathway at 0 K is the addition of HO• to the terminal carbon atom of the C═C double bond through a transition-state structure lying 0.7 kcal/mol below the energy of the reactants. The other pathway leads to the HO• addition to the central carbon atom of the C═C double bond via a transition-state structure lying 0.8 kcal/mol above the energy of the reactants. In good agreement with available experimental data, the rate coefficients at 298 K calculated for these HO• addition reactions lead to a branching ratio of about 95:5.

(4) The sum of the rate coefficients at 298 K calculated for the three reaction pathways studied is found to be 0.77304 $\times$ 10^{-11} molecule^{-1} cm^{-3} s^{-1}. This value is roughly in reasonable agreement with the reported experimental rate coefficients. Furthermore, the rate coefficients at 298 K calculated for the three reaction pathways lead to a branching ratio of about 75:24:1, which is in good agreement with available experimental data.

Acknowledgment. This research was supported by the Spanish MEC (Grant CTQ2005-07790-C02-01). Additional support came from the Catalonian AGAUR (Grant 2005SGR00111 and 2005PEIR0051/69). The larger calculations described in this work were performed at the Centre de Supercomputació de Catalunya (CESCA).

Supporting Information Available: Table summarizing total energies, zero-point vibrational energies, and thermal corrections to enthalpy and Gibbs energy as well as the Cartesian coordinates of all structures reported in this paper. This material is available free of charge via the Internet at http://pubs.acs.org.

References

(1) Grosjean, D. J. *Air Waste Manage. Assoc.* **1990**, *40*, 1664–1668.

(2) Tuazon, E. C.; Alvarado, A.; Aschmann, S. M.; Atkinson, R.; Arey, J. *Environ. Sci. Technol.* **1999**, *33*, 3586.

(3) Liu, X.; Jefries, H. E.; Sexton, K. G. *Atmos. Environ.* **1999**, *33*, 3005.

(4) Berndt, T.; Böge, O. *J. Phys. Chem. A* **2007**, *111*, 12099–12105.

(5) Agency for Toxic Substances and Disease Registry (ATSDR). Toxicological Profile for Acrolein, U.S. Public Health Service; U.S. Department Health and Human Services: Atlanta, GA, 1989.

(6) Maldotti, A.; Chiorboli, C.; Bignozzi, C. A.; Bartocci, C.; Carassiti, V. *Int. J. Chem. Kinet.* **1980**, *12*, 905–913.

(7) Kerr, J. A.; Sheppard, D. W. *Environ. Sci. Technol.* **1981**, *15*, 960–963.

(8) Atkinson, R.; Aschmann, S. M.; Pitts, J. N. *Int. J. Chem. Kinet.* **1983**, *15*, 75–81.

(9) Edney, E. O.; Kleindienst, T. E.; Corse, E. W. *Int. J. Chem. Kinet.* **1986**, *18*, 1355–1371.

(10) Magneron, I.; Thévenet, R.; Mellouki, A.; Le Bras, G.; Moortgat, G. K.; Wirtz, K. *J. Phys. Chem. A* **2002**, *106*, 2526–2537.

(11) Grosjean, E.; Williams, E. L.; Grosjean, D. *Total Environ.* **1994**, *153*, 195–202.

(12) Orlando, J. J.; Tyndall, G. S. *J. Phys. Chem. A* **2002**, *106*, 12252–12259.

(13) In addition to the low-energy pathways associated with reactions of eqs 1–3, which occur under atmospheric conditions, high-energy pathways could take place at high temperatures. For instance, the direct HO• abstraction of olefinic H-atoms of acrolein leading to different substituted vinyl radicals plus H_2O might play an important role in combustion processes. Although there are not experimental data on these hypothetical reaction pathways, it is worthy to note that the energy barrier for H-atom abstraction from ethylene is 4.9 kcal/mol.[14] Since the energy barriers found for the pathways associated with reactions of eqs 1–3 range between −1.1 and 0.8 kcal/mol, it can be concluded that the reaction pathways for direct HO• abstraction of olefinic H-atoms of acrolein are unimportant under atmospheric conditions.

(14) Senosiain, J. P.; Klippenstein, S. J.; Miller, J. A. *J. Phys. Chem. A* **2006**, *110*, 6960–6970.

(15) Pople, J. A.; Head-Gordon, M.; Raghavachari, K. *J. Chem. Phys.* **1987**, *87*, 5968.

(16) Kendall, R. A.; Dunning, T. H., Jr.; Harrison, R. J. *J. Chem. Phys.* **1992**, *96*, 6796.

(17) (a) Fukui, K. *Acc. Chem. Res.* **1981**, *14*, 363. (b) Ishida, K.; Morokuma, K.; Kormornicki, A. *J. Chem. Phys.* **1977**, *66*, 2153.

(18) (a) Gonzalez, C.; Schlegel, H. B. *J. Chem. Phys.* **1989**, *90*, 2154. (b) Gonzalez, C.; Schlegel, H. B. *J. Phys. Chem.* **1990**, *94*, 5523.

(19) Knowles, P. J.; Hampel, C.; Werner, H.-J. *J. Chem. Phys.* **1993**, *99*, 5219.

(20) (a) Purvis, G. D.; Bartlett, R. J. *J. Chem. Phys.* **1982**, *76*, 1910. (b) Hampel, C.; Peterson, K. A.; Werner, H.-J. *Chem. Phys. Lett.* **1992**, *190*, 1. (c) Deegan, M. J. O.; Knowles, P. J. *Chem. Phys. Lett.* **1994**, *227*, 321.

(21) For a review, see: Bartlett, R. J. *J. Phys. Chem.* **1989**, *93*, 1967.

(22) Raghavachari, K.; Trucks, G. W.; Pople, J. A.; Head-Gordon, M. *Chem. Phys. Lett.* **1989**, *157*, 479.

(23) Mayer, P. M.; Parkinson, C. J.; Smith, D. M.; Radom, L. *J. Chem. Phys.* **1998**, *108*, 604–615.

(24) Senosiain, J. P.; Miller, J. A. *J. Phys. Chem. A* **2007**, *111*, 3740–3747.

(25) Lynch, B. J.; Fast, P. L.; Harris, M.; Truhlar, D. G. *J. Chem. Phys.* **1998**, *108*, 604–615.

(26) See, e.g., McQuarrie, D. *Statistical Mechanics*; Harper and Row: New York, 1986.

(27) Boys, S. F.; Bernardi, F. *Mol. Phys.* **1970**, *19*, 553.

(28) (a) Bader, R. F. W. *Atoms in Molecules: A Quantum Theory;* Clarendon: Oxford, U.K., 1990. (b) Matta C. F.; Boyd R. J. An Introduction to the Quantum Theory of Atoms in Molecules. In *The Quantum Theory of Atoms in Molecules,* 1st ed.; Matta, C. F., Boyd, R. J., Eds.; Wiley-VCH: Weinheim, Germany, 2007; pp 1−34.

(29) Mulliken, R. S. *J. Chem. Phys.* **1955**, *23*, 1833.

(30) See e.g. Wiberg, K. B.; Hadad, C. M.; LePage, T.; Breneman, C. M.; Frisch, M. J. *J. Phys. Chem.* **1992**, *96*, 671.

(31) Frisch, M. J. ; Trucks, G. W.; Schlegel, H. B.; Scuseria, G. E.; Robb, M. A.; Cheeseman, J. R.; Montgomery, J. A.; Jr.;

Vreven, T.; Kudin, K. N.; Burant, J. C.; Millam, J. M.; Iyengar, S. S.; Tomasi, J.; Barone, V.; Mennucci, B.; Cossi, M.; Scalmani, G.; Rega, N.; Petersson, G. A.; Nakatsuji, H.; Hada, M.; Ehara, M.; Toyota, K.; Fukuda, R.; Hasegawa, J.; Ishida, M.; Nakajima, T.; Honda, Y.; Kitao, O.; Nakai, H.; Klene, M.; Li, X.; Knox, J. E.; Hratchian, H. P.; Cross, J. B.; Adamo, C.; Jaramillo, J.; Gomperts, R.; Stratmann, R. E.; Yazyev, O.; Austin, A. J.; Cammi, R.; Pomelli, C.; Ochterski, J. W.; Ayala, P. Y.; Morokuma, K.; Voth, G. A.; Salvador, P.; Dannenberg, J. J.; Zakrzewski, V. G.; Dapprich, S.; Daniels, A. D.; Strain, M. C.; Farkas, O.; Malick, D. K.; Rabuck, A. D.; Raghavachari, K.; Foresman, J. B.; Ortiz, J. V.; Cui, Q.; Baboul, A. G.; Clifford, S.; Cioslowski, J.; Stefanov, B. B.; Liu, G.; Liashenko, A.; Piskorz, P.; Komaromi, I.; Martin, R. L.; Fox, D. J.; Keith, T.; Al-Laham, M. A.; Peng, C. Y.; Nanayakkara, A.; Challacombe, M.; Gill, P. M. W.; Johnson, B.; Chen, W.; Wong, M. W.; Gonzalez, C.; Pople, J. A. *GAUSSIAN 03 (Revision C.02)*; Gaussian, Inc.: Wallingford, CT, 2004.

(32) Werner, H.-J.; Knowles, P. J.; Almlöf, J.; Amos, R. D.; Berning, A.; Cooper, D. L.; Deegan, M. J. O.; Dobbyn, A. J.; Eckert, S. T.; Hampel, C.; Leininger, C.; Lindh, R.; Lloyd, A. W.; Meyer, W.; Mura, M. E.; Nicklass, A.; Palmieri P.; Peterson, K. A.; Pitzer, R.; Pulay, P.; Rauhaut, G.; Schütz, M.; Stoll, H.; Stone, A. J.; Thorsteinsson, T. *MOLPRO, version 98.1*; University of Stuttgart: Germany, 1998.

(33) (a) Biegler-König, F. W.; Bader, R. F. W.; Tang, T.-H. *J. Comput. Chem.* **1982**, *3*, 317. (b) Bader, R. F. W.; Tang, T.-H.; Tal, Y.; Biegler-König, F. W. *J. Am. Chem. Soc.* **1982**, *104*, 946.

(34) Singleton, D. L.; Cvetanovic, R. J. *J. Am. Chem. Soc.* **1976**, *98*, 6812.

(35) Eyring, H. *J. Chem. Phys.* **1935**, *107*, 107.

(36) Truong, T. N.; Truhlar, D. G. *J. Chem. Phys.* **1990**, *93*, 1761.

(37) Eckart, C. *Phys. Rev.* **1930**, *35*, 1303.

(38) Alvarez-Idaboy, J. R.; Mora-Diez, N.; Boyd, R. J.; Vivier-Bunge, A. *J. Am. Chem. Soc.* **2001**, *123*, 2018.

(39) Hehre, W. J.; Radom, L.; Schleyer, P. v. R.; Pople, J. A. *Ab Initio Molecular Orbital Theory*; John Wiley: NY, 1986; pp 86−87.

(40) Atkinson, R.; Baulch, D. L.; Cox, R. A.; Hampson, R. F.; Kerr, J. A.; Rossi, M. J.; Troe, J. *J. Phys. Chem. Ref. Data* **1999**, *28*, 191.

(41) (a) Cremer, D. *Croat. Chem. Acta* **1984**, *57*, 1259. (b) Cremer, D. *Angew. Chem., Int. Ed. Engl.* **1984**, *23*, 627.

CT8000798